

Statistical fluctuations in laser transients

S. Zhu, A. W. Yu, and R. Roy

School of Physics, Georgia Institute of Technology, Atlanta, Georgia 30332

(Received 4 June 1986)

Laser fluctuations are measured and characterized with a new technique based on the concept of first-passage-time distributions. This first-passage-time technique makes it possible to discern quantum noise in a dye laser even in the presence of pump fluctuations that are many orders of magnitude larger. We report new analytic and experimental results for the mean, variance, and skewness of the first-passage-time distributions. The analytic results agree well with numerical computations and experimental measurements. Our technique is particularly suited to the quantitative description of laser fluctuations above threshold; it complements the conventional photoelectric counting and correlation methods which are valuable for lasers below and near threshold but are difficult to implement for lasers far above threshold. The limits of validity of the theory containing a cubic nonlinearity are examined in the context of passage-time measurements. The effects of multiplicative noise and saturation on the variance of the intensity fluctuations are also discussed. A new signature of multiplicative noise is predicted.

I. INTRODUCTION

Statistical fluctuations in laser radiation determine the limits on the use of lasers in almost every application. The information transmission rates in optical communications, the accuracy of optical computing techniques, and the reliability of spectroscopic data are all crucially dependent on and limited by the amplitude and phase fluctuations present in laser light. While lasers are operated far above threshold in practically every application, previous studies of laser fluctuations have focused on operation below or slightly above threshold.¹⁻⁴

To characterize the fluctuations of laser light far above threshold one must examine the effects of intrinsic quantum noise due to spontaneous emission and also of "pump" noise due to external sources. In this paper we describe the use of a novel technique based on the concept of first-passage-time (FPT) distributions to describe the statistical fluctuations of a laser. These are the distributions of times taken by the laser to develop from spontaneous emission to a given value of the intensity, under the influence of both quantum and pump noise sources. The technique requires fast photodiodes and simple electronics; it complements the standard but delicate photoelectron counting and correlation methods which remain valuable near threshold. In contrast to the difficulties encountered in the latter methods, fluctuations in lasers pumped high above threshold are easily measured and the effects of quantum noise and pump fluctuations are clearly distinguished by the FPT measurements. In the experiments described here on ring dye lasers, the measured FPT distributions enable us to determine the time scale and magnitude of external pump noise and quantum fluctuations (which are almost 8 orders of magnitude smaller than the pump noise) much more efficiently than has been possible with other methods.

The time development of laser radiation is initially

dominated by spontaneous emission. Only fully quantum-mechanical or augmented semiclassical laser theories provide an adequate theoretical framework for the description of this process. By "augmented" we mean those theories where spontaneous emission is accounted for by appropriate Langevin sources in an otherwise semiclassical theory. The basic approaches to laser theory have been comprehensively presented by Haken;¹ Sargent, Scully, and Lamb;² and by Lax³ and Louisell.⁴ The results of the augmented semiclassical and fully quantized theories have been shown to be extremely close; both predict the same statistical features of the laser radiation for a single-mode laser model.

The single-mode laser theories¹⁻⁴ have been successful in describing the experimental results of Arecchi and co-workers⁵ and of Meltzer and Mandel⁶ on transients in He-Ne lasers. Their elegant photon-counting experiments measured the growth of the mean intensity with time, and the development of the variance of the photon number with time. Arecchi, Mandel, and others (see Refs. 1-4 for reviews) have also performed detailed measurements on the photon statistics and intensity correlations of the light from single-mode He-Ne lasers operating in the steady state. Satisfactory agreement with theory was obtained.

Recently, it has become clear that parametric (pump) fluctuations can affect the steady-state fluctuations and correlations in a rather drastic way. Experiments on dye lasers^{7,8} showed that the conventional laser theory¹⁻⁴ which contains only quantum noise fails to predict the statistical properties of light from these lasers. The subsequent theoretical developments by Schenzle and Graham,^{9,10} Sancho, San Miguel, and their colleagues,^{11,12} Dixit and Sahni,¹³ Fox, James, and Roy,^{14,15} Lindenberg, West, and Cortes,¹⁶ Jung and Risken,¹⁷ and others have examined the importance of pump fluctuations in laser systems.

While all the work mentioned so far concentrates on the

calculation of photon statistics and correlations, there has been much interest expressed recently in the calculation of first passage times in lasers and other systems. Gordon and Aslaksen,¹⁸ Suzuki,¹⁹ Haake, Haus, and Glauber,^{20,21} Arecchi and Politi,^{22,23} Young and Singh,²⁴ and de Pasquale, Tartaglia, and Tombesi^{25,26} have examined the first-passage-time problem with additive (quantum) noise only. Polder *et al.*²⁷ and Goy *et al.*²⁸ have examined the question in the context of superfluorescence and Rydberg masers.

We should point out that the concept of first-passage-time distributions is not new; it has a long and distinguished history. Schrödinger,²⁹ Kramers,³⁰ Darling and Siegert,³¹ Montroll and Shuler,³² Landauer and Swanson,³³ Stratonovich,³⁴ and Weiss³⁵ have contributed to the theory of first-passage-time problems in different areas of physics and chemistry. The recent texts of Van Kampen,³⁶ Schuss,³⁷ Gardiner,³⁸ and Risken³⁹ give very readable treatments of the passage-time problem.

Several recent treatments of FPT problems address the question of colored (non- δ -correlated) additive and multiplicative noise. Hanggi, Moss, and co-workers,^{40,41} Fox,^{42,43} Masoliver, Lindenberg, and West,⁴⁴ and de Pasquale *et al.*⁴⁵ have developed the theory of stochastic processes driven by noise sources with nonzero correlation times. References 43 and 45(b) are concerned directly with the first-passage-time problem for the laser, and contain analytic results for the mean and variance of the FPT distributions measured experimentally and computed numerically in Ref. 46.

In this paper we present the results of first-passage-time measurements on a single-mode dye ring laser, and compare the experimental observations to the predictions of theoretical models. In Sec. II we describe the laser system and measurement techniques used. Two theoretical models, the first with additive noise only, and the second with both additive and multiplicative noise, are described in Sec. III. In Sec. IV we survey the available analytic results on FPT distributions and present new analytic results for a model with both additive and multiplicative noise. The techniques used for numerical computations are discussed in Sec. V, and a comparison of the analytic, numerical, and experimental results is presented. The models considered so far are based on the third-order Lamb theory of the laser; in Sec. VI the limits of this theory are examined in the context of FPT measurements. Section VII describes the effects of multiplicative noise on the laser intensity fluctuations in the transient regime. Saturation effects on the statistics are also considered. A discussion of the present status of theory and experiment concludes the paper.

II. EXPERIMENTAL APPARATUS

The experiments were performed on a single-mode, unidirectional ring dye laser (Fig. 1) that is extremely stable in steady-state operation. The laser is mounted on a vibration-isolated table and contained within a dust-free enclosure. A Pellin-Broca prism and coated etalons maintain single-mode operation. This is monitored constantly with a confocal Fabry-Perot interferometer. A Faraday

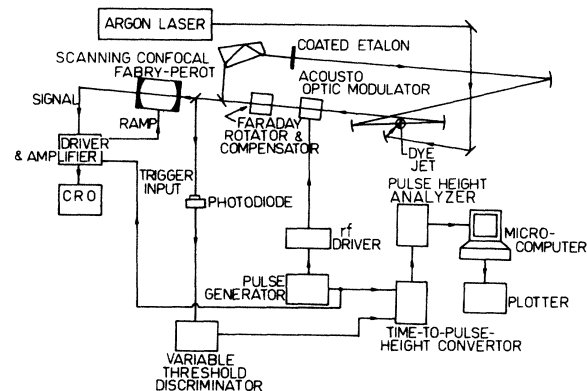


FIG. 1. Apparatus for passage-time distribution measurements.

rotator and compensator are used to obtain unidirectional operation of the laser. The length of the ring cavity is 160 cm and the round-trip loss per pass is $\sim 12\%$.

An acousto-optic modulator (AOM) in the laser cavity is used to turn the laser on and off. The time required for the modulator to go from maximum transmission (2% insertion loss) to the maximum loss condition (60% diffraction efficiency) requires ~ 15 ns, which is much shorter than the time scale for the growth of the laser field to the steady state. A pulse generator is used to turn the laser on; it takes several microseconds to reach the steady state with a mean intensity I_{ss} . The laser is allowed to stay on for about 600 μ s. It is then turned off for about 400 μ s. This process is repeated several hundred thousand times.

The laser output beam is incident on a fast photodiode with a rise time of ~ 1 ns and a linear response over several decades of intensity. As the laser is turned on with the AOM, a trigger pulse marks the beginning of the turn-on time. The laser intensity $I(t)$ develops from a random, spontaneous emission background. When the intensity crosses a reference value I_{ref} the photodiode voltage crosses a preset threshold on the discriminator and a pulse is generated. The initial trigger pulse and this pulse are the start and stop inputs for a time-to-pulse-height converter which generates an output pulse with amplitude proportional to the separation in time between the start and stop pulses. These output pulses are measured by a pulse-height analyzer which then generates the passage-time distribution for the growth of the laser radiation.

In the context of conventional laser fluctuation studies,¹⁻⁴ a pump power 1% above the threshold value is considered "far" above threshold. Fluctuations in the intensity (root mean square) due to quantum noise are already reduced to less than 0.01% of the steady-state average intensity. In our experiments the laser was operated up to $\sim 20\%$ above threshold.

A microcomputer, interfaced to the pulse-height analyzer, was used for storage and analysis of the data. The 1024 data channels of the pulse-height analyzer provide adequate resolution in time. A zero calibration is necessary for the output of the time-to-pulse-height

converter. Such corrections were included in the computer program used for the data analysis.

The experimental measurements of the first-passage-time distributions were performed after the laser had been operating for several hours, and experimental conditions were thermally and mechanically stable. The laser was adjusted to operate in a single longitudinal mode, which was monitored constantly with the confocal Fabry-Perot. More than 20 such measurements were made over a two-hour period, with the laser about 6% above threshold. The measurements published earlier⁴⁶ were made with the laser about 20% above threshold. It is extremely important to operate the laser in a clean, single longitudinal mode during the measurements. The presence of additional modes or significant mode-hopping results in FPT distributions with multiple peaks. These will be the subject of a later study.

The FPT distributions show a progressive shift to the right as the reference intensity is increased, i.e., the laser takes a longer time to reach a higher intensity. The distributions also grow in width and develop a decided asymmetry. We will quantify our discussion of these three features by calculating the mean, variance, and skewness of the FPT distributions. We note here that the measurements of the skewness are extremely sensitive to points in the tail of the distribution. These measurements are thus susceptible to the largest errors.

An important precaution in these measurements is to ensure that the acousto-optic modulator turns the laser off completely before letting it turn on again. This requires that it is aligned accurately for maximum diffraction efficiency (60%), thus ensuring that the laser is far below threshold before it is Q switched. We also note that the pump laser is always maintained constant in our measurements. Thermal stability of the dye is thus maintained, and we do not have to consider the time taken to create a population inversion. This issue has been discussed in some detail in Ref. 5.

III. THEORETICAL MODELS

Model A: Additive noise. The conventional theoretical model for a single-mode laser contains only quantum noise. Spontaneous emission is included in a density-matrix formalism through the quantization of the electromagnetic radiation field. Equations of motion for the diagonal elements of the field density operator are derived which describe the development in time of the laser intensity.¹⁻⁴ The results of such a model have been demonstrated to be equivalent to those obtained from an augmented semiclassical theory. The third-order Lamb theory equation of motion for the complex electric field E is augmented by the addition of a Langevin noise term, as shown below:

$$dE/dt = aE - A|E|^2E + q(t) \quad (1)$$

with

$$\langle q_i(t)q_j(t') \rangle = P\delta_{ij}\delta(t-t') \quad (i,j=1,2), \quad (2)$$

where a and A are the net gain and self-saturation coefficients, and $q(t)$ is a complex, δ -correlated, Gaussian noise source which represents the effect of spontaneous emission on the field E . Until very recently, this model was the basis for calculations of laser fluctuations in the steady state¹⁻⁴ and in transients.^{1-6,18-26}

The actual electric field E' has been scaled as follows,²

$$E = \frac{1}{2} \left[\frac{\mu^2}{\hbar^2 \gamma_a \gamma_b} \right]^{1/2} E', \quad (3)$$

to render it dimensionless. Here μ is the dipole moment of the laser transition and γ_a and γ_b are the lifetimes of the upper and lower lasing levels. Other scale factors have been used by various authors;¹⁻⁴ this is largely a matter of individual preference and convenience.

The statistics of the laser field may be determined from Eqs. (1) and (2) by converting them to a Fokker-Planck equation for the probability function $Q(E,t)$.^{1-4,34,36-39} The mean, variance, and higher moments may be obtained from the steady-state probability distribution for the field, while the time-dependent solution of the Fokker-Planck equation is essential for the correlation functions of the field. The time-dependent solutions also provide the statistics of the laser field during the period of transient growth from a spontaneous emission background.

The passage-time calculations in Refs. 18-26 apply to this model of the laser. In Sec. V we will review some of the analytic results available for FPT distributions based on this laser model.

Model B: Additive and multiplicative noise. The experiments described in Refs. 7 and 8 demonstrated that the conventional laser model was not adequate to describe the steady-state statistics or correlation functions of single-mode dye lasers. It soon became clear that parametric fluctuations played an important role in the fluctuations of these lasers,⁹⁻¹⁷ and thus a new source of external "pump" noise must be included in order to obtain a realistic statistical description of these lasers. While a microscopic density-matrix approach to such pump fluctuations is available^{14,15} it is perhaps most convenient for calculations to utilize the counterparts of Eqs. (1) and (2) given below:

$$dE/dt = a_0E - A|E|^2E + p(t)E + q(t), \quad (4)$$

$$dp(t)/dt = -\gamma p(t) + \gamma q'(t) \quad (5)$$

with

$$\langle q'_i(t)q'_j(t') \rangle = P'\delta_{ij}\delta(t-t') \quad (i,j=1,2) \quad (6)$$

which implies

$$\langle p_i(t)p_j(t') \rangle = \frac{P'\gamma}{2} e^{-\gamma|t-t'|}, \quad \gamma \equiv 1/\tau \quad (7)$$

while Eq. (2) remains unchanged.

In this model, the net gain a , previously assumed constant, is considered a stochastic quantity. Thus the net

gain is $a_0 + p(t)$, where a_0 is the average net gain and $p(t)$ is the pump noise term. Instead of taking $p(t)$ to be δ correlated, Eqs. (5)–(7) allow us to assign a time scale $(1/\gamma)$ to the pump fluctuations. The pump noise is thus described by an Ornstein-Uhlenbeck process with an exponential correlation function.

The $p(t)$ noise term accounts for fluctuations in the net gain of the laser. These fluctuations may arise from turbulence in the dye jet, or from pump laser noise.⁴⁶ In the dye laser, the magnitude of the pump fluctuations may be far larger than the quantum noise. The steady-state photon statistics and correlation functions will thus be totally dominated by the pump noise. The experimental measurements^{7,8} have been satisfactorily explained by theoretical treatments which contain only pump noise.^{9–17}

It is of great interest to attempt to disentangle the effects of quantum noise and pump noise. Clearly, from Eq. (4), the $p(t)E$ term contributes but little when the field is in its initial stage of growth. At that time it is the quantum spontaneous emission noise which is the dominant factor. One is thus likely to discern the effects of quantum noise if measurements are performed on the transient growth of the laser intensity. It is possible to examine the effects of additive and multiplicative noise on the moments of the transient laser intensity,⁴⁵ or instead examine the passage-time distributions as we have done in our measurements. Even though the main emphasis here will be on FPT distributions we will examine the effect of the multiplicative noise on the moments of the transient intensity in Sec. VII.

IV. ANALYTIC RESULTS ON FIRST-PASSAGE-TIME DISTRIBUTIONS

The two models described in Sec. III have been used to calculate the first-passage-time distributions. While most of the analyses use model A with additive (spontaneous emission) noise only,^{18–26} some efforts have very recently been made to obtain the FPT distributions for model B with both quantum and pump noise.^{43,45} We apply the technique developed by Haake, Haus, and Glauber²¹ first to model A and obtain analytic approximate expressions for the FPT distribution and its mean and variance. The results of de Pasquale *et al.*,^{45(b)} based on a linearized analysis of the two-dimensional problem with additive and multiplicative colored noise, are reviewed. We also describe the one-dimensional analysis of Fox⁴³ which contains both additive and multiplicative noise. Finally, we present a new two-dimensional treatment of the FPT problem for model B which includes nonlinear effects. The results from these various theoretical analyses are compared to the results of experiments and numerical simulations in the next section.

A. Theory of Haake, Haus, and Glauber (Ref. 21)

This theory may be directly applied to the equations of motion for the laser field [Eqs. (1) and (2)] with δ -correlated additive white noise. The FPT distribution obtained from the application of their theory is

$$W(t) = \frac{2a_0^2 I_{\text{ref}} e^{-2a_0 t} \left[1 - \frac{AI_{\text{ref}}}{a_0} \right]}{P(1 - e^{-a_0^2/PA}) \left[1 - \frac{AI_{\text{ref}}}{a_0} (1 - e^{-a_0 t}) \right]^2} \times \exp \left[\frac{-a_0 I_{\text{ref}} e^{-2a_0 t}}{P \left[1 - \frac{AI_{\text{ref}}}{a_0} (1 - e^{-2a_0 t}) \right]} \right], \quad (8)$$

where I_{ref} is the reference intensity of the laser field and $a = a_0$ in Eq. (1). The moment generating function²¹ of $W(t)$ is of the form

$$\begin{aligned} \tilde{W}(\lambda) &= \int_0^\infty dt e^{-\lambda t} W(t) \\ &\simeq \frac{a_0^2 e^{-a_0^2/PA}}{PA(1 - e^{-a_0^2/PA})} \left[\frac{a_0}{AI_{\text{ref}}} \left[1 - \frac{AI_{\text{ref}}}{a_0} \right] \right]^{(\lambda/2a_0)} \\ &\quad \times B(1 - \lambda/2a_0, 1 + \lambda/2a_0) \\ &\quad \times {}_1F_1(1 - \lambda/2a_0; 2; a_0^2/PA), \end{aligned} \quad (9)$$

where B is the beta function and ${}_1F_1$ is the degenerate hypergeometric function.⁴⁷ Differentiating Eq. (9) we obtain after lengthy calculations the mean first-passage time

$$\langle t \rangle_H \simeq \frac{1}{2a_0} \left[C + \ln \left[\frac{a_0^2}{PA} \right] + \ln \left[\frac{I_0}{1 - I_0} \right] \right], \quad (10)$$

the variance

$$\langle (\Delta t)^2 \rangle_H \simeq (\pi^2/24a_0^2), \quad (11)$$

and the coefficient of skewness

$$\frac{\langle (t - \langle t \rangle_H)^3 \rangle_H}{\langle (\Delta t)^2 \rangle_H^{3/2}} \simeq 2 \left[\frac{\sqrt{6}}{\pi} \right]^3 \sum_{l=1}^\infty \frac{1}{l^3} \simeq 1.14, \quad (12)$$

where $C = 0.5772 \dots$ is Euler's constant and $I_0 \equiv AI_{\text{ref}}/a_0$ is the reference intensity normalized by the semiclassical steady-state intensity $I_{\text{ss}} = a_0/A$.

B. Linear approximation of de Pasquale *et al.* [Ref. 45(b)]

A formal analytic solution for the laser intensity has been obtained by de Pasquale, Sancho, San Miguel, and Tartaglia^{45(b)} for the model in Eqs. (4)–(7). It is

$$I(t) = \frac{|h(t)|^2 e^{2[a_0 t + V(t)]}}{1 + 2A |h(t)|^2 \int_0^t dt' e^{2[a_0 t' + V(t')]}}, \quad (13)$$

where

$$h(t) = \int_0^t dt' e^{-a_0 t'} q(t') \quad (14)$$

and

$$V(t) = \int_0^t dt' \text{Re}[p(t')] . \quad (15)$$

In the linear regime which corresponds to an intensity range beyond the immediate vicinity of the initial unstable state and also far from the final equilibrium state, Eq. (13) is approximated by

$$I(t) \simeq |h|^2 e^{2[a_0 t + V(t)]} . \quad (16)$$

In the absence of pump noise ($P'=0$), the asymptotic value of the mean first-passage time is

$$T_0 = \frac{1}{2a_0} \ln \left[\frac{a_0 I_{\text{ref}}}{P} \right] . \quad (17)$$

When the correlation time τ is short ($\tau \ll t$), an approximate passage-time generating function is

$$W(\lambda) = \frac{\Gamma(\lambda/2a_0 + 1) e^{-\lambda T_0}}{\left[1 + \frac{\lambda P'}{a_0^2} \right]^{1/2}} \exp \left[\frac{\lambda^2 (T_0 - \tau) P'}{2a_0^2 \left[1 + \frac{\lambda P'}{a_0^2} \right]} \right] , \quad (18)$$

where $\Gamma(x)$ denotes the gamma function. From this generating function it follows that

$$\langle t \rangle_P \simeq \frac{1}{2a_0} \left[C + \frac{P'}{a_0} + \ln \left[\frac{a_0^2}{PA} \right] + \ln I_0 \right] \quad (19)$$

and

$$\langle (\Delta t)^2 \rangle_P \simeq \frac{\pi^2}{24a_0^2} + \frac{P'}{2a_0^3} \left\{ \left[\frac{P'}{a_0} + \ln \left[\frac{a_0^2}{PA} \right] - 2a_0 \tau \right] + \ln I_0 \right\} . \quad (20)$$

C. One-dimensional approximation of Fox (Ref. 43)

If the complex field E is expressed as $E = x e^{i\phi}$, a one-dimensional contracted model may be obtained,

$$\frac{dx}{dt} = a_0 x - Ax^3 + x \text{Re}(p) + \text{Re}(q) , \quad (21)$$

where the correlations of q and p are given in Eqs. (2) and (7). For short correlation times τ (compared to the times of observation) of the pump noise $p(t)$, an effective Fokker-Planck equation is obtained⁴² for the probability function $Q(x, t)$,

$$\frac{\partial Q}{\partial t} = - \frac{\partial}{\partial x} (FQ) + \frac{\partial^2}{\partial x^2} (DQ) , \quad (22)$$

where

$$F(x) = a_0 x - Ax^3 + P' F_1(x)/2 , \quad (23)$$

$$D(x) = P/2 + P' x F_1(x)/2 , \quad (24)$$

and

$$F_1(x) = \frac{x(1 - 2a_0 \tau) + 4A\tau x^3}{[1 - \tau(a_0 - 3Ax^2)]^2} . \quad (25)$$

If the laser field begins with $x=0$ and the intensity reaches the reference value I_{ref} , the mean first-passage time and its variance are given by⁴⁸

$$\langle t(0, I_{\text{ref}}^{1/2}) \rangle = \int_0^{I_{\text{ref}}^{1/2}} dx \int_0^x dz \frac{1}{D(z)} \exp[-U(x) + U(z)] \quad (26)$$

and

$$\begin{aligned} \langle (\Delta t)^2(0, I_{\text{ref}}^{1/2}) \rangle &= \langle t(0, I_{\text{ref}}^{1/2}) \rangle^2 \\ &\quad - 2 \int_0^{I_{\text{ref}}^{1/2}} dx \int_0^x dz \frac{\langle t(0, z) \rangle}{D(z)} \\ &\quad \times \exp[-U(x) + U(z)] \end{aligned} \quad (27)$$

in which

$$U(x) = \int^x dz \frac{F(z)}{D(z)} . \quad (28)$$

If the correlation time τ is very small (multiplicative white noise), the approximate mean first-passage time and the variance are given by

$$\langle t \rangle_F \simeq \frac{1}{2a_0} \left[C + \ln \left[\frac{2a_0^2}{PA} \right] + \ln \left[\frac{I_0}{1 - I_0} \right] \right] \quad (29)$$

and

$$\begin{aligned} \langle (\Delta t)^2 \rangle_F &\simeq \frac{\ln 2}{a_0^2} + \frac{P'}{2a_0^3} \left\{ \left[C - \frac{5}{2} + \ln \left[\frac{a_0^2}{PA} \right] \right] \right. \\ &\quad \left. + \frac{\frac{3}{2} - I_0}{(1 - I_0)^2} + \ln \left[\frac{I_0}{1 - I_0} \right] \right\} . \end{aligned} \quad (30)$$

D. Model with additive and multiplicative white noise

In this section we give analytic results for the mean and variance of the FPT distributions obtained by a somewhat different technique than those of Refs. 21, 43, and 45. We note that the colored nature of the multiplicative noise plays a role only in the results of Ref. 45, which, however, employs a linearized treatment. If we let $\gamma \rightarrow \infty$ in Eq. (7), we obtain the limit in which the colored noise $p(t)$ is replaced by white noise.

The details of the derivation are given in the Appendix. Here, we observe that if one integrates over the phase, the Fokker-Planck equation for $Q(x, t)$, the probability func-

tion, may be written

$$\begin{aligned} \frac{\partial Q}{\partial t} = & -\frac{\partial}{\partial x} \left[\left(a_0 x - Ax^3 + \frac{P}{2x} + \frac{1}{2}P'x \right) Q \right] \\ & + \frac{1}{2} \frac{\partial^2}{\partial x^2} [(P + P'x^2)Q]. \end{aligned} \quad (31)$$

Here $E = E_1 + iE_2$ is the laser field, $E_1 = x \cos\phi$, and

$E_2 = x \sin\phi$, and P and P' are the strengths of the additive and multiplicative white noise sources.

If the laser field starts initially from $x = 0$ and arrives at a reference value $x = I_{\text{ref}}^{1/2}$, the mean and variance of the FPT distribution are given by²³

$$\langle t \rangle = \int_0^{I_{\text{ref}}^{1/2}} dx \frac{1}{V(x)} \int_0^x dy \frac{V(y)}{D(y)} \quad (32)$$

$$\langle (\Delta t)^2 \rangle = 4 \int_0^{I_{\text{ref}}^{1/2}} dx \frac{1}{V(x)} \int_0^x dy \frac{1}{V(y)} \int_0^y d\xi \frac{V(\xi)}{D(\xi)} \int_0^\xi d\eta \frac{V(\eta)}{D(\eta)}, \quad (33)$$

where

$$V(x) = e^{U(x)}, \quad U(x) = \int^x \frac{F(\eta)}{D(\eta)} d\eta, \quad (34)$$

$$F(x) = a_0 x - Ax^3 + \frac{P}{2x} + \frac{1}{2}P'x, \quad (35)$$

and

$$D(x) = \frac{1}{2}(P + P'x^2). \quad (36)$$

These multiple integrals [Eqs. (32) and (33)] may be evaluated approximately as shown in the Appendix to give

$$\langle t \rangle \simeq \frac{1}{2a_0} \left[C + \ln \left[\frac{a_0^2}{PA} \right] + \ln \left[\frac{I_0}{1-I_0} \right] \right] \quad (37)$$

and

$$\begin{aligned} \langle (\Delta t)^2 \rangle \simeq & \frac{\pi^2}{24a_0^2} + \frac{P'}{2a_0^3} \left[\left(\frac{3}{2} - I_0 \right) / (1 - I_0)^2 + \ln \left[\frac{I_0}{1 - I_0} \right] \right. \\ & \left. - \frac{3}{2} + \ln(4 \times 10^6) + \ln \left[\frac{a_0}{A} \right] \right]. \end{aligned} \quad (38)$$

In the next section we compare these analytic results with numerical computations and with experimental measurements.

V. NUMERICAL SIMULATIONS: COMPARISON OF THEORY AND EXPERIMENT

It is necessary to perform numerical calculations to obtain the FPT distributions and its moments; we can check the accuracy of the analytic approximations and also obtain fits to the experimental data.

The numerical procedure followed to obtain FPT distributions is that of Monte Carlo simulations. Equations (1), (2), and (4)–(7) may be integrated step by step,^{11(a)} noting the value of the intensity I of the field after each step. As soon as $I > I_{\text{ref}}$, the number of the time step is stored.

Gaussian random numbers are generated to simulate the Langevin force terms at each integration step. This procedure was repeated ten thousand times to construct the FPT distributions.

In Fig. 2 we show three typical stochastic trajectories obtained by this integration procedure. This illustrates the nature of growth of the laser intensity in some particular realizations of the random process. The stochastic behavior of the intensity after it reaches the plateau is due almost entirely to the multiplicative noise term.

Two sets of experimental data have been compared with the theoretical results. Set A was taken with the laser operating about 6% above threshold and set B at about 20% above threshold.⁴⁶ We show in Fig. 3 the measured FPT distributions together with those obtained from the simulations performed as described in the previous section, for the first set of data. The experimental measurements have been fit by the same values of constants a_0 , A , P , P' , and γ . The constants are obtained by varying them until the simulated distributions match the measured ones, and are quite reasonable in value. The parameters are $a_0 = 0.7 \times 10^6 \text{ s}^{-1}$, $A = 0.114 \times 10^6 \text{ s}^{-1}$, $P = 0.004$

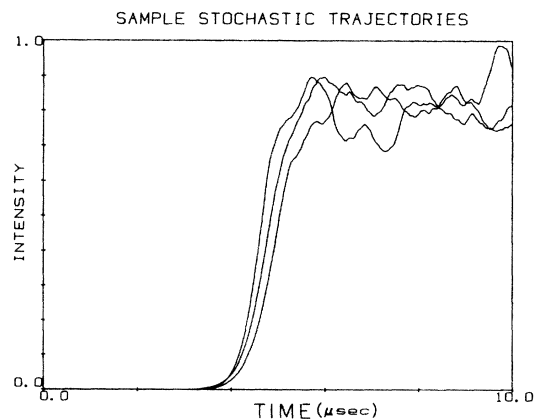


FIG. 2. Sample stochastic trajectories generated by Monte Carlo simulations of Eqs. (4)–(7).

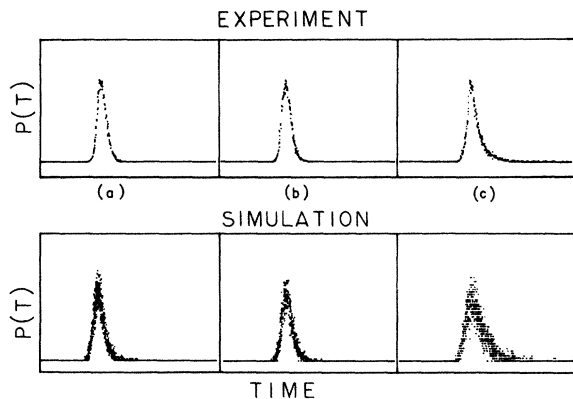


FIG. 3. Comparison of measured passage-time distributions with the results of Monte Carlo simulations of a single-mode laser model with quantum fluctuations and pump noise. (a) $I_{\text{ref}}/I_{\text{ss}}=0.236$, (b) $I_{\text{ref}}/I_{\text{ss}}=0.66$, (c) $I_{\text{ref}}/I_{\text{ss}}=0.99$. The laser parameters are kept constant for all the computations: $a_0=0.7 \times 10^6 \text{ s}^{-1}$, $A=0.114 \times 10^6 \text{ s}^{-1}$, $P=0.004 \text{ s}^{-1}$, $P'=10^4 \text{ s}^{-1}$, $\gamma=2 \times 10^6 \text{ s}^{-1}$, and the total time scale is $37.26 \mu\text{s}$.

s^{-1} , $P'=10^4 \text{ s}^{-1}$, and $\gamma=2 \times 10^6 \text{ s}^{-1}$ and are determined to about 20% accuracy.

We note that the parameters a_0 and A can be independently estimated from measurements of the cavity loss, pump power above threshold, and known decay rates of the Rhodamine 6G molecule.⁴⁹ Thus it is the parameters P , P' , and γ which are freely varied to fit the distributions. The large “noise” in the simulated distributions is due to the fact that 10 000 stochastic trajectories were computed whereas several hundred thousand were measured experimentally for each distribution of passage times.

A large number of FPT distributions were measured for set A, since the laser is somewhat unstable when operated close to threshold. The data were taken over a period of several hours, during which thermal drifts were inevitable. We have plotted the mean, variance, and skewness obtained from the 23 measurements of FPT distributions. These are shown in Fig. 4.

The mean of the set-A FPT distributions has been plotted as a function of $I_0=(I_{\text{ref}}/I_{\text{ss}})$ in Fig. 4(a). The data have been fit by the numerical simulations containing both additive and multiplicative noise. The same values of the parameters (given above) have been used for all the simulations in this set. The curves obtained from the analytic results are also shown. Equations (10) and (37) are identical and show good agreement with the experimental and numerical results, as does Eq. (29), over the entire range of values of $(I_{\text{ref}}/I_{\text{ss}})$. The results for the linear approximation, Eq. (19), show reasonable agreement for $0 < I_{\text{ref}}/I_{\text{ss}} < 0.7$; the agreement is not so good in the regime when the cubic nonlinearity is important. The role of multiplicative noise is minimal in determination of the mean first-passage time. In fact, the numerical simulations reveal that the mean passage times with and without multiplicative noise are indistinguishable from each other

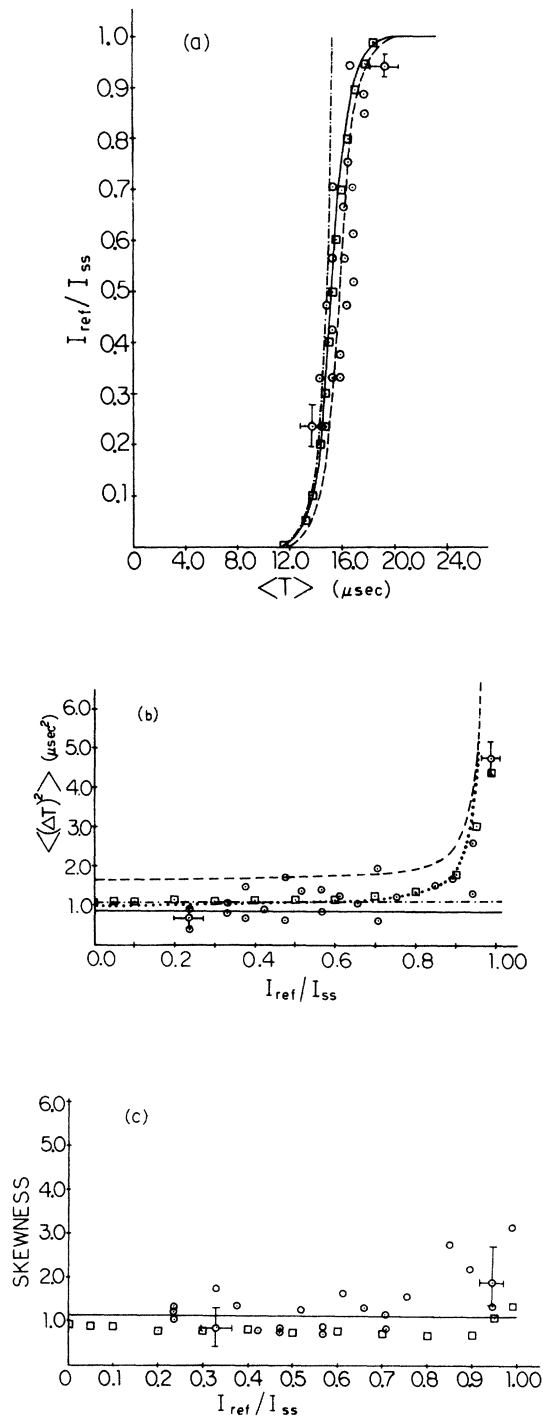


FIG. 4. (a) Mean first-passage times for set A, with the laser $\sim 6\%$ above threshold. \odot , experimental measurements; \square , numerical simulations; —, Eqs. (10) and (37); — — —, Eq. (29); — · — · —, Eq. (19). The laser parameters are those given for Fig. 3. (b) Variance of the FPT distributions (set A). \odot , experimental measurements; \square , numerical simulations; —, Eq. (11) (only additive noise); — · — · —, Eq. (20) (linearized treatment); — — —, Eq. (30) (one-dimensional treatment); · · · · ·, Eq. (38). The laser parameters are those given for Fig. 3. (c) Coefficient of skewness $\langle (t - \langle t \rangle)^3 \rangle / (\langle \Delta t^2 \rangle)^{3/2}$ (set A). \odot , experimental measurements; \square , numerical simulations; —, Eq. (12) (additive noise only). The laser parameters are those given for Fig. 3.

on the scale of the figure.

The variance [Fig. 4(b)] of the FPT distributions reveals several interesting features. Even with the scatter in the data, it is clear that the variance shows a systematic increase as $I_{\text{ref}}/I_{\text{ss}}$ approaches unity. [The result for the model with only additive noise, Eq. (11), does not display this increase; neither does Eq. (20), obtained from the linearized theory.] It is therefore clear that both multiplicative noise and the nonlinear terms are essential to obtain reasonable agreement with experimental measurements. We note that Eq. (20) gives good agreement with the simulations and experiment for $0 < I_{\text{ref}}/I_{\text{ss}} < 0.7$, i.e., in the regime of validity claimed by the authors.⁴⁵ Equation (30) predicts a somewhat high value of the variance for

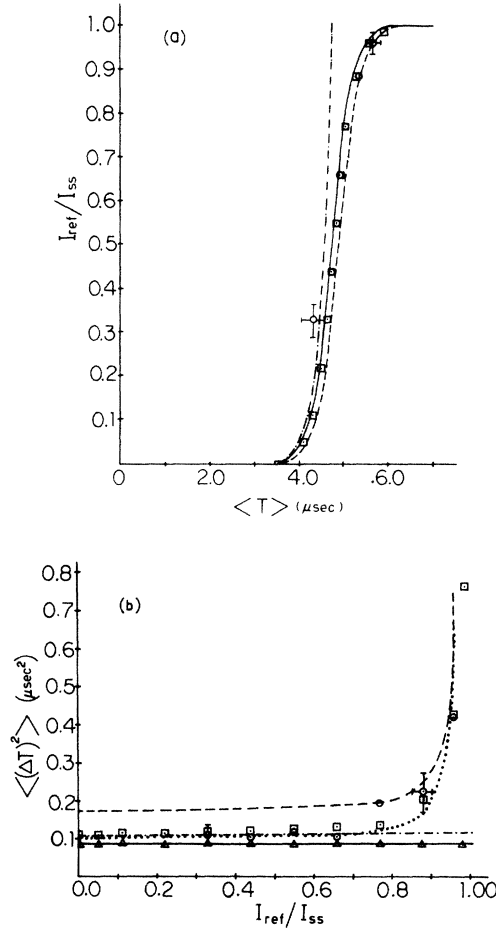


FIG. 5. (a) Mean first-passage times for set B ($\sim 20\%$ above threshold). \odot , experimental measurements; \square , numerical simulations; —, Eqs. (10) and (37); — — —, Eq. (29); — · — · —, Eq. (19). $a_0 = 2.16 \times 10^6 \text{ s}^{-1}$, $A = 2.64 \times 10^6 \text{ s}^{-1}$, $P = 0.0043 \text{ s}^{-1}$, $P' = 3 \times 10^4 \text{ s}^{-1}$, and $\gamma = 2.4 \times 10^6 \text{ s}^{-1}$ are the laser parameters. (b) Variance of the FPT distributions (set B). \odot , experimental measurements; \triangle , numerical simulations with additive noise only; \square , numerical simulations with additive and multiplicative noise. —, Eq. (11); — · — · —, Eq. (20); — — —, Eq. (30); · · · · ·, Eq. (38). The laser parameters are the same as for Fig. 5(a).

small $I_{\text{ref}}/I_{\text{ss}}$, but the curve shows the increase in the variance seen in the experiments and computations. The best overall agreement is clearly obtained with Eq. (38), which agrees quite well with the data and simulations over the entire range.

Figure 4(c) shows the skewness of the FPT distributions of set A. The scatter in the data is quite large, but still indicates clearly that the skewness remains constant until $I_{\text{ref}}/I_{\text{ss}}$ is quite close to unity. The skewness is subject to a large uncertainty, since a couple of data points in the tails of the distributions are sufficient to produce considerable changes in its value. We find that the data is fit quite well by Eq. (12), i.e., the constant value 1.14. The numerical simulations with the same values of parameters as used to fit the mean and variance give a value which appears to be slightly low.

Figures 5(a) and 5(b) show the mean and variance of the FPT distributions of set B.⁴⁶ The values of the parameters are $a_0 = 2.16 \times 10^6 \text{ s}^{-1}$, $A = 2.64 \times 10^6 \text{ s}^{-1}$, $\gamma = 2.4 \times 10^6 \text{ s}^{-1}$, $P = 0.0043 \text{ s}^{-1}$, and $P' = 3 \times 10^4 \text{ s}^{-1}$.

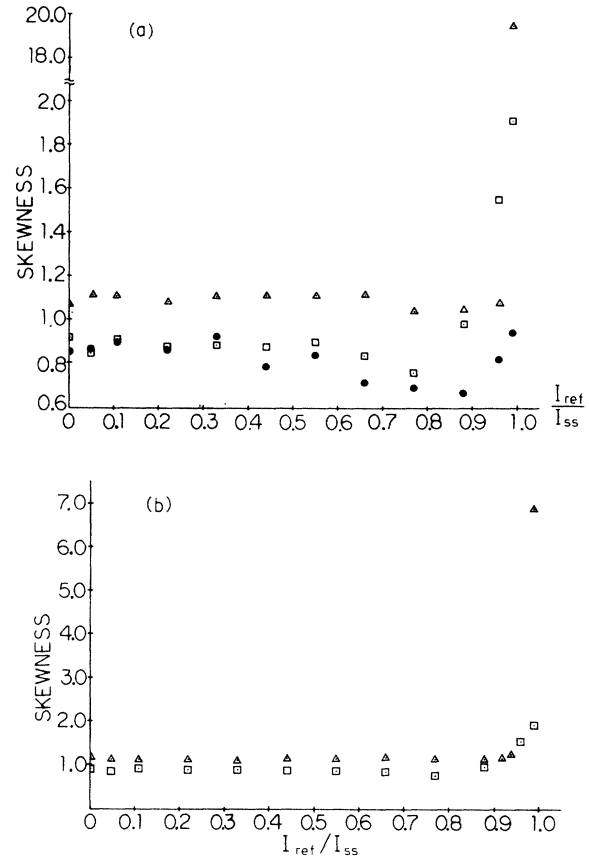


FIG. 6. (a) Dependence of the coefficient of skewness on the time scale of the colored multiplicative noise. \triangle , $\gamma = 2.4 \times 10^4 \text{ s}^{-1}$; \square , $\gamma = 2.4 \times 10^6 \text{ s}^{-1}$; \bullet , $\gamma = 2.4 \times 10^7 \text{ s}^{-1}$. The other parameters are those for the set-A data ($\sim 6\%$ above threshold). (b) Dependence of the coefficient of skewness on the time scale of the colored multiplicative noise. \triangle , $\gamma = 2.4 \times 10^4 \text{ s}^{-1}$; \square , $\gamma = 2.4 \times 10^6 \text{ s}^{-1}$. The other parameters are those for the set-B data.

We note that the values of P , P' , and γ used for sets A and B are quite close to each other. This points to the consistency of the entire procedure of measurements and calculations, since the experiments were performed after a total realignment of the laser cavity. The differences in a_0 and A are largely due to the difference in pump power for the two sets of data. A factor which may contribute to additional differences in operating parameters is a difference in operating wavelengths. Once again, it is interesting to compare the analytic results to the experimental data and the simulations. This is shown in Fig. 5; the behavior is similar to that already noted in the discussion of set A.

We have also examined the effect of changing γ , the time scale of the fluctuations, on the skewness. This is

shown in Fig. 6. It is seen that the skewness decreases as γ is increased. The shorter the time scale of the pump fluctuations, the less skewed is the distribution of the first-passage times. The curves all show an upward trend for values of $I_{\text{ref}}/I_{\text{ss}}$ close to 1. Figure 6(b) examines the dependence of the skewness on γ for the parameter values used for set B.

VI. SATURATION EFFECTS: LIMITS OF THIRD-ORDER THEORY

The models described in Sec. III both contain only cubic nonlinearities; the theory thus includes saturation effects to third order in the field. We investigate in this section and the next the limitations of the third-order

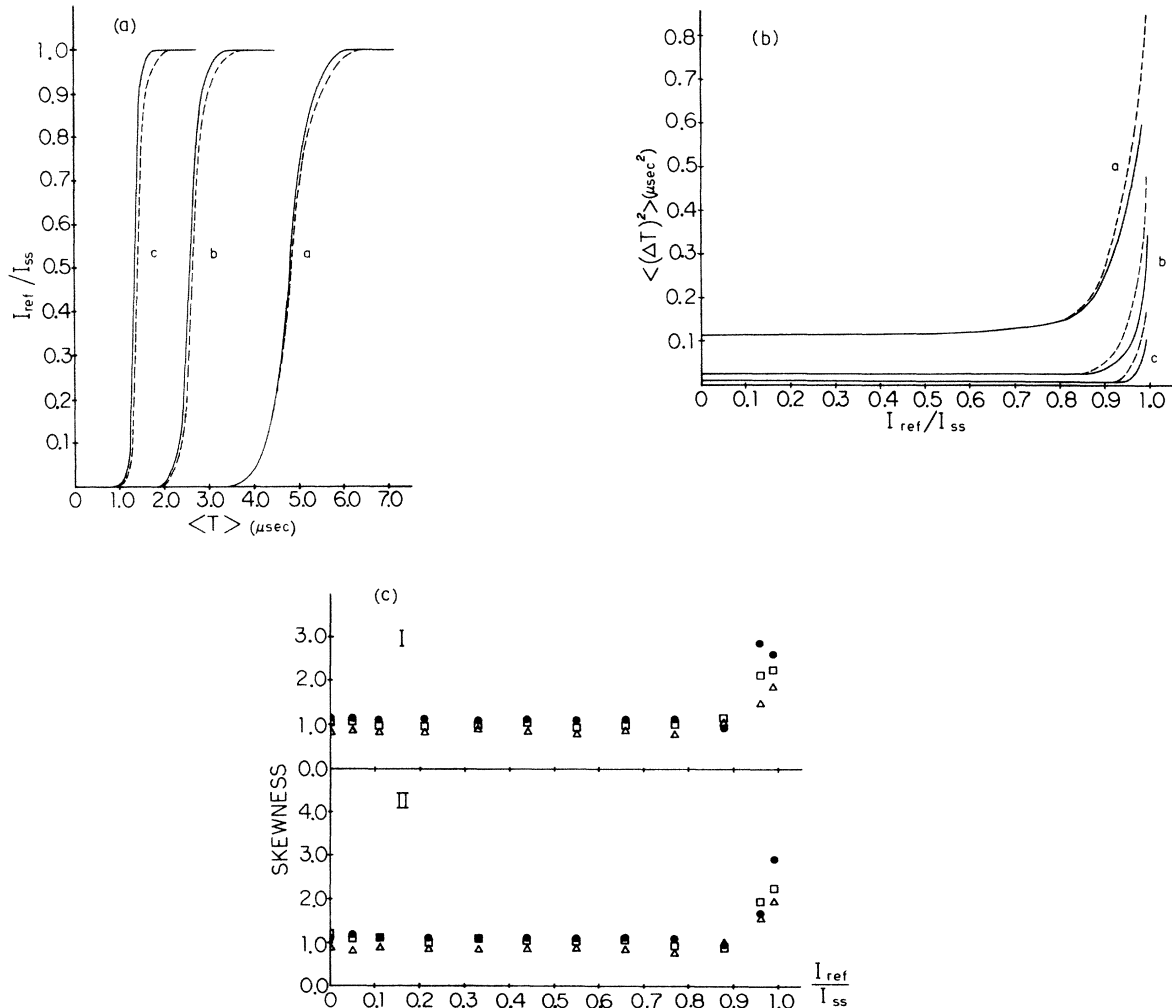


FIG. 7. (a) The effect of saturation [Eq. (39)] on the mean first-passage time. —, cubic nonlinearity [Eq. (4)]; - - -, Eq. (39). Curve a, $a_0 = 2.16 \times 10^6 \text{ s}^{-1}$; Curve b, $a_0 = 4.32 \times 10^6 \text{ s}^{-1}$; Curve c, $a_0 = 8.64 \times 10^6 \text{ s}^{-1}$. The effect of saturation is prominent at the higher excitation. The other laser parameters are those of set B. (b) The effect of saturation on the variance of the FPT distributions. —, cubic nonlinearity [Eq. (4)]; - - -, Eq. (39). Curve a, $a_0 = 2.16 \times 10^6 \text{ s}^{-1}$; Curve b, $a_0 = 4.32 \times 10^6 \text{ s}^{-1}$; Curve c, $a_0 = 8.64 \times 10^6 \text{ s}^{-1}$. The other laser parameters are those of set B. (c) Graph labeled I is skewness coefficient for FPT distributions based on Eq. (39). Δ , $a_0 = 2.16 \times 10^6 \text{ s}^{-1}$; \square , $a_0 = 4.32 \times 10^6 \text{ s}^{-1}$; \bullet , $a_0 = 8.64 \times 10^6 \text{ s}^{-1}$. Graph labeled II is skewness coefficient for FPT distributions based on Eq. (4). The other laser parameters are those of set B.

theory—often called the cubic model.

A fuller account of the saturation properties of the laser may be obtained from the following equation:¹⁻⁴

$$dE/dt = -KE + \frac{FE}{1 + \frac{A}{F}I} + p(t)E + q(t), \quad (39)$$

with Eqs. (2) and (5)–(7) to describe the noise sources. $K = 1.2 \times 10^7 \text{ s}^{-1}$ is the cavity decay rate, $F = a_0 + K$ is the gain factor, and A is the laser saturation parameter. A simple binomial expansion of the denominator leads to the cubic model.

The experiments performed until now have been within the regime of validity of the cubic model. Thus, in this section we will compare the results obtained from computer simulations of Eqs. (4) and (39). Calculations of the FPT distributions have been performed for the pump excitation of Ref. 46 and also for twice and four times as much above threshold. The values of the other parameters A , K , P , P' , and γ have been kept the same, in order to provide a direct comparison.

The curves in Fig. 7(a) show the mean FPT for the three pump levels. For the original set of parameter values [curves *a*] the percentage difference between the cubic and saturation models is extremely small, and would also be indistinguishable in an experiment. As we go to the higher values of excitation [curves *b* and *c*], the percentage difference grows progressively larger, and becomes quite noticeable in the curves *c*.

Figures 7(b) and 7(c) show the variance and skewness for the cubic and saturation models for the three levels of excitation. These figures once again demonstrate that given the accuracy of the data that are available so far, the cubic model gives a good representation of the fluctuations for the levels of excitation at which the experiments have been performed.

At present, there are no analytic results available for the FPT distribution or its moments that use Eq. (39), to our knowledge. It should be mentioned that the steady-state photon statistics for a laser with only quantum noise have been calculated² taking into account saturation effects of the form shown in Eq. (39).

We also note that Schenzle^{10(b)} has considered the effect of both loss and gain fluctuations on the laser field variance and correlation functions, but with only multiplicative noise present.

VII. EFFECT OF MULTIPLICATIVE NOISE ON INTENSITY FLUCTUATIONS

In the previous sections of this paper we have reported on the effect of multiplicative noise on the passage time statistics. The “signature” of pump (multiplicative) noise was found to be the rapid increase in the variance of the FPT distributions. In this section we examine in some detail the effect of the multiplicative noise on the mean and variance of the laser intensity in the transient regime.

Calculations of the variance of the laser intensity have been performed by de Pasquale *et al.*^{45(a)} on a one-dimensional laser model and more recently^{45(b)} also on the model in Eqs. (4)–(7). The calculations presented here

have been done on Eqs. (4)–(7) as well; we examine three different levels of excitation, as in the last section, and point out saturation effects. However, we have also discovered from our computations an alternative signature of pump fluctuations if one normalizes the time-dependent variance of the intensity fluctuations by the

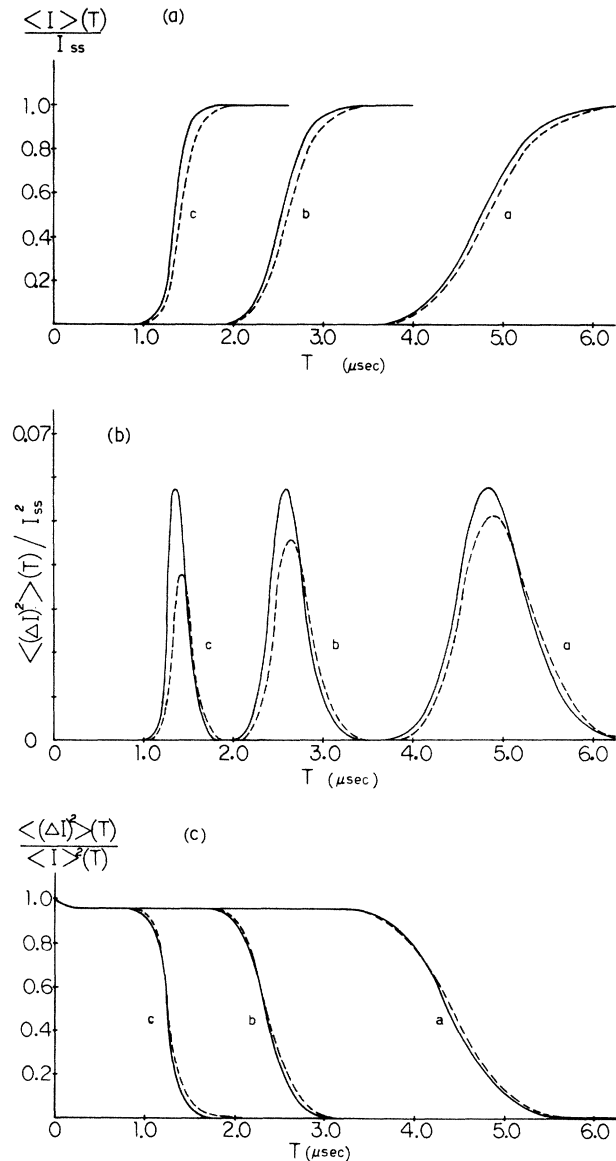


FIG. 8. (a) The time-dependent mean intensity for the laser transients. Curves *a*, *b*, and *c* correspond to the three values of a_0 used in Fig. 7. —, cubic nonlinearity [Eq. (1)]; — — —, Eq. (39). Only additive noise is included. (b) The time-dependent variance of the intensity fluctuations, normalized by I_{ss} . Curves *a*, *b*, and *c* correspond to three different values of a_0 , as in Fig. 7. —, cubic nonlinearity [Eq. (1)]; — — —, Eq. (39). Only additive noise is included. (c) The time-dependent variance of the intensity fluctuations, normalized by the time-dependent mean intensity. The curves *a*, *b*, and *c* correspond to three different values of a_0 , as in Fig. 7. —, cubic nonlinearity [Eq. (1)]; — — —, Eq. (39). Only additive noise is included.

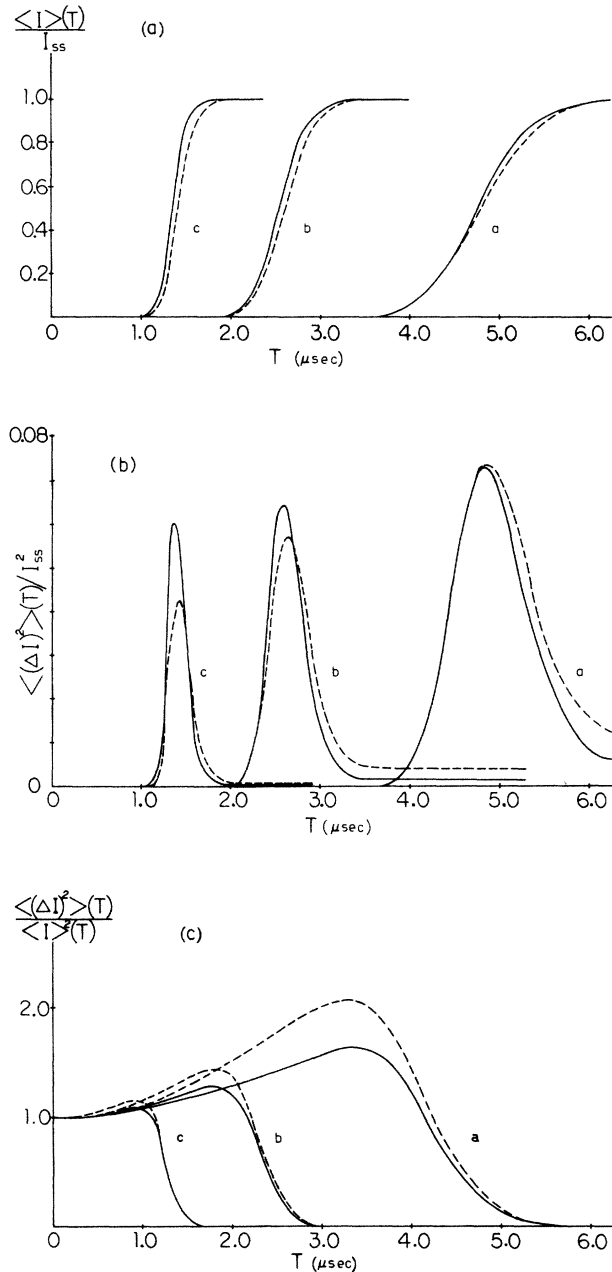


FIG. 9. (a) The time-dependent mean intensity for the laser transients. The curves *a*, *b*, and *c* correspond to the three different values of a_0 used in Fig. 7. —, cubic nonlinearity [Eq. (4)]; — —, Eq. (39). Both additive and multiplicative noise are now included. (b) The time-dependent variance of the intensity fluctuations, normalized by I_{ss}^2 . Curves *a*, *b*, and *c* correspond to three different values of a_0 , as in Fig. 7. —, cubic nonlinearity [Eq. (4)]; — —, Eq. (39). Both additive and multiplicative noise are now included. (c) The time-dependent variance of the intensity fluctuations normalized by the time-dependent mean intensity. Curves *a*, *b*, and *c* correspond to the three different values of a_0 used in Fig. 7. —, cubic nonlinearity [Eq. (4)]; — —, Eq. (39). Both additive and multiplicative noise are now included. The relative intensity fluctuations now exceed unity before decreasing to the steady-state values; this is a clear indication of multiplicative noise [compare with Fig. 8(c)].

time-dependent intensity. This will be described in detail below.

Figure 8 shows the results of calculations on the cubic model and Eq. (39) with additive noise only. The effects of saturation are clearly visible in the graphs and increase in percentage as the level of excitation above threshold is increased. In these plots we have normalized the mean and variance of the intensity in different ways. In Figs. 8(a) and 8(b), I_{ss} (the steady-state average intensity) has been used for normalization. The curves in Fig. 8(c) are very similar to those of de Pasquale *et al.*,²⁵ in addition we see the saturation effects, which clearly play a major role in curves *b* and *c*, as the level of excitation is increased.

In Fig. 8(c), the normalization is with respect to the time-dependent mean intensity. In this case, $\langle(\Delta I)^2\rangle(t)/\langle I\rangle^2(t)$ decreases from the initial value of unity to the steady-state value. The initial value of unity is, of course, what one would expect of thermal light. The curves thus show the transition from thermal to laser statistics. We note that $\langle(\Delta I)^2\rangle(t)/\langle I\rangle^2(t)$ never increases above unity for this case, which just contains additive noise.

Figure 9 is based on Eqs. (4)–(7), which contain both additive and multiplicative noise. Figures 9(a) and 9(b), normalized by the steady-state average intensity I_{ss} , once again demonstrate the effects of saturation beyond the cubic model. The effects of the multiplicative noise are clear in Fig. 9(b) where the steady-state relative intensity fluctuations are seen to have a far greater value than in Fig. 8(b). Also apparent is the large effect of saturation relative to the cubic model. The predicted relative intensity fluctuations in the steady state in Fig. 9(b) are almost twice that for the cubic model.

In Fig. 9(c) the intensity fluctuations are normalized by the time-dependent average intensity. There is now a clear and unambiguous sign of multiplicative noise: $\langle(\Delta I)^2\rangle(t)/\langle I\rangle^2(t)$ now *exceeds unity*, the effect increasing as the laser is operated closer to threshold. It is also important to note that the relative fluctuations are considerably larger if the saturation effects are accounted for more fully than in the cubic model.

VIII. DISCUSSION

The analysis of laser fluctuations based on measurements of first-passage-time distributions is examined and shown to be a very powerful technique capable of detecting the presence of quantum fluctuations that are many orders of magnitude smaller than the pump fluctuations. The magnitude and time scale of the pump fluctuations can also be determined. The technique is implemented with a photodiode and simple electronics, and is particularly suited for the study of fluctuations in lasers operated far above threshold. This is in contrast to the conventional but delicate photon-counting and correlation techniques, which remain valuable below and near threshold.

The analytic results presented in this paper are in good agreement with the results of the experiments and numerical computations. We note that the theory could be further improved if both the nonlinearity in the equations of

motion for the laser field and the colored nature of the multiplicative noise could be incorporated in the analytic treatment. The limits of the third-order theory have been examined numerically, and its predictions are found to agree well with the high-intensity form of the laser equations in the regime of the experiments. However, deviations are evident at higher values of excitation above threshold.

We also consider the intensity fluctuations of the laser in the transient regime. We find a new indicator of the presence of multiplicative noise; the variance of the intensity fluctuations normalized by the time-dependent mean intensity exceeds unity temporarily when multiplicative noise is present. It would be of great interest to verify this feature experimentally.

The present technique should be easily applicable to the analysis of fluctuations in a variety of single-mode laser systems; in particular, it appears that semiconductor-laser fluctuations could be characterized conveniently by this method. Some progress has already been made in the calculation of switching transients in semiconductor lasers.^{50,51} Such measurements of FPT statistics for semiconductor lasers would be of importance in optical communications.

The existence of two or more longitudinal laser modes may lead to multiple peaks in the FPT distributions. This has been experimentally observed.⁵² We will report on this in a future publication.

In conclusion, we have developed a new technique for the measurement and analysis of laser fluctuations that is particularly useful for lasers operated above threshold.

ACKNOWLEDGMENTS

We thank Ron Fox for many valuable suggestions and discussions of his theoretical analysis (Ref. 43). It is a pleasure to acknowledge discussions with Surendra Singh and Maxi San Miguel, who also sent us reports of Refs. 45(a) and 45(b) prior to publication. We are grateful to Joe Haus for discussions and the communication of his unpublished results. We are indebted to Enrique Peacock and Katja Lindenberg for a correction to the original manuscript and for several helpful discussions. This research was supported in part by a Cottrell Research Grant. This paper is based on a thesis submitted by S. Z. in partial fulfillment of the requirements for the Ph.D. degree at the Georgia Institute of Technology.

APPENDIX: DERIVATION OF EQS. (31), (37), and (38)

If the field E is written as $E = E_1 + iE_2$, Eq. (4) may be separated into real and imaginary parts as follows:

$$\dot{E}_1 = a_0 E_1 - A |E|^2 E_1 + E_1 p_1 - E_2 p_2(t) + q_1(t), \quad (\text{A1})$$

$$\dot{E}_2 = a_0 E_2 - A |E|^2 E_2 + E_1 p_2 + E_2 p_1(t) + q_2(t). \quad (\text{A2})$$

Letting $\gamma \rightarrow \infty$ in Eq. (7) we obtain the limit in which the colored noise is replaced by white noise. We now have

$$\langle p_i(t) p_j(t') \rangle = P' \delta_{ij} \delta(t - t') \quad (i, j = 1, 2) \quad (\text{A3})$$

and

$$\langle p_i(t) \rangle = 0 \quad (i = 1, 2). \quad (\text{A4})$$

The Fokker-Planck equation corresponding to Eqs. (A1)–(A4) for \tilde{Q} , the probability density function, is found to be³⁹

$$\begin{aligned} \frac{\partial \tilde{Q}}{\partial t} = & - \sum_{i=1}^2 \frac{\partial}{\partial E_i} \left\{ \left[a_0 - A \left(\sum_{i=1}^2 E_i^2 \right) \right] E_i \tilde{Q} \right\} \\ & + \frac{1}{2} \sum_{i=1}^2 \frac{\partial^2}{\partial E_i^2} \left\{ \left[P + P' \left(\sum_{i=1}^2 E_i^2 \right) \right] \tilde{Q} \right\}, \end{aligned} \quad (\text{A5})$$

where $E = E_1 + iE_2$ is the laser field.

The use of polar coordinates

$$E_1 = x \cos \phi, \quad (\text{A6})$$

$$E_2 = x \sin \phi, \quad (\text{A7})$$

with

$$\bar{Q} = x \tilde{Q} \quad (\text{A8})$$

leads to the Fokker-Planck equation

$$\begin{aligned} \frac{\partial \bar{Q}}{\partial t} = & - \frac{\partial}{\partial x} \left[\left(a_0 x - A x^3 + \frac{P}{2x} + \frac{1}{2} P' x \right) \bar{Q} \right] \\ & + \frac{1}{2} \frac{\partial^2}{\partial x^2} [(P + P' x^2) \bar{Q}] + \left[\frac{P + P' x^2}{2x^2} \right] \frac{\partial^2 \bar{Q}}{\partial \phi^2}. \end{aligned} \quad (\text{A9})$$

Since we are interested in measuring the intensity of the single-mode laser field, we integrate over the phase in Eq. (A9), to obtain [with $Q = \int_0^{2\pi} \bar{Q}(x, \phi) d\phi$]

$$\begin{aligned} \frac{\partial Q}{\partial t} = & - \frac{\partial}{\partial x} \left[\left(a_0 x - A x^3 + \frac{P}{2x} + \frac{1}{2} P' x \right) Q \right] \\ & + \frac{1}{2} \frac{\partial^2}{\partial x^2} (P + P' x^2) Q. \end{aligned} \quad (\text{A10})$$

If the laser field starts initially from $x = 0$ and arrives at a reference value $x = I_{\text{ref}}^{1/2}$, the mean and variance of the FPT distribution are given by²³

$$\langle t \rangle = \int_0^{I_{\text{ref}}^{1/2}} dx \frac{1}{V(x)} \int_0^x dy \frac{V(y)}{D(y)} \quad (\text{A11})$$

and

$$\langle (\Delta t)^2 \rangle = 4 \int_0^{I_{\text{ref}}^{1/2}} dx \frac{1}{V(x)} \int_0^x dy \frac{1}{V(y)} \int_0^y d\xi \frac{V(\xi)}{D(\xi)} \int_0^\xi d\eta \frac{V(\eta)}{D(\eta)}, \quad (\text{A12})$$

where

$$V(x) = e^{U(x)}, \quad U(x) = \int^x d\eta \frac{F(\eta)}{D(\eta)}, \quad (\text{A13})$$

$$F(x) = a_0 x - Ax^3 + \frac{P}{2x} + \frac{1}{2}P'x, \quad (\text{A14})$$

and

$$D(x) = \frac{1}{2}(P + P'x^2). \quad (\text{A15})$$

We separate the calculation of $\langle t \rangle$ and $\langle (\Delta t)^2 \rangle$ into two

regimes; $0 < x < 5 \times 10^{-4}$ and $5 \times 10^{-4} < x < (I_{ss})^{1/2}$ (with $I_{ss} = a_0/A$, since the two terms in $D(x)$ [Eq. (A15)] are approximately equal for $x = 5 \times 10^{-4}$. Equations (A11) and (A12) may be written as

$$\langle t \rangle = \int_0^{5 \times 10^{-4}} dx \frac{1}{V(x)} \int_0^x dy \frac{V(y)}{D(y)} + \int_{5 \times 10^{-4}}^{I_{ss}^{1/2}} dx \frac{1}{V(x)} \int_0^x dy \frac{V(y)}{D(y)} \quad (\text{A16})$$

and

$$\begin{aligned} \langle (\Delta t)^2 \rangle = & 4 \int_0^{5 \times 10^{-4}} dx \frac{1}{V(x)} \int_0^x dy \frac{1}{V(y)} \int_0^y d\xi \frac{V(\xi)}{D(\xi)} \int_0^\xi d\eta \frac{V(\eta)}{D(\eta)} \\ & + 4 \int_{5 \times 10^{-4}}^{I_{ss}^{1/2}} dx \frac{1}{V(x)} \int_0^x dy \frac{1}{V(y)} \int_0^y d\xi \frac{V(\xi)}{D(\xi)} \int_0^\xi d\eta \frac{V(\eta)}{D(\eta)}. \end{aligned} \quad (\text{A17})$$

For $0 < x < 5 \times 10^{-4}$, i.e., $0 < I_{ref} < 2.5 \times 10^{-7}$, the additive quantum noise dominates the growth of the field. We may thus neglect the multiplicative noise term and cubic term in Eqs. (A14) and (A15) and get

$$F(x) \simeq a_0 x + \frac{P}{2x} \quad (0 < x < 5 \times 10^{-4}) \quad (\text{A18})$$

$$D(x) \simeq \frac{P}{2} \quad (0 < x < 5 \times 10^{-4}). \quad (\text{A19})$$

Also,

$$U(x) \simeq \frac{a_0 x^2}{P} + \ln x, \quad (\text{A20})$$

$$V(x) = e^{U(x)} \simeq x e^{a_0 x^2/P}. \quad (\text{A21})$$

Therefore, we have,⁴⁷ for the first integral in Eq. (A16),

$$\begin{aligned} & \int_0^{5 \times 10^{-4}} dx \frac{1}{V(x)} \int_0^x dy \frac{V(y)}{D(y)} \\ & \simeq \frac{1}{2a_0} \left[\ln(2.5 \times 10^{-7}) + C + \ln \left[\frac{a_0}{P} \right] \right], \end{aligned} \quad (\text{A22})$$

where C is Euler's constant. As we will see $a_0/P \sim 10^8$, which is typical for a wide variety of lasers, and hence we approximate $e^{-x^2 a_0/P} \simeq 0$. For the variance, Eq. (A17), we may similarly evaluate the first part of Eq. (A17),

$$\begin{aligned} & 4 \int_0^{5 \times 10^{-4}} dx \frac{1}{V(x)} \int_0^x dy \frac{1}{V(y)} \int_0^y d\xi \frac{V(\xi)}{D(\xi)} \int_0^\xi d\eta \frac{V(\eta)}{D(\eta)} \\ & \simeq \frac{1}{a_0^2} \int_0^{5 \times 10^{-4}} dx \frac{e^{-a_0 x^2/P}}{x} \left[\epsilon_i \left[\frac{a_0 x^2}{P} \right] - \epsilon_i \left[\frac{-a_0 x^2}{P} \right] \right] \\ & \quad + \frac{2}{a_0^2} \int_0^{5 \times 10^{-4}} dx \frac{e^{-a_0 x^2/P}}{x} \left[\epsilon_i \left[-\frac{a_0 x^2}{P} \right] - C - \ln \left[\frac{a_0 x^2}{P} \right] \right] \\ & \simeq \frac{1}{2a_0^2} \sum_{k=1}^{\infty} \frac{1}{k(k!)} \int_0^{\infty} dz e^{-z} [z^{k-1} - (-1)^{k-1} z^{k-1}] \\ & = \frac{1}{2a_0^2} \left[\sum_{k=1}^{\infty} \frac{1}{k^2} - \sum_{k=1}^{\infty} \frac{(-1)^{k-1}}{k^2} \right] \\ & = \frac{\pi^2}{24a_0^2}, \end{aligned} \quad (\text{A23})$$

where we have used ϵ_i , the exponential integral function.⁴⁷

The domain of interest is $x \in (0, I_{ss}^{1/2})$. In this domain $F(x)$ and $D(x)$ are positive, which means $U(x)$ is monotone increasing. The monotone behavior of $U(x)$ and its large size in most of the x domain (for typical values of the parameters) allow us to expand the exponential of $V(y)/D(y)$ around x for $x \in (5 \times 10^{-4}, I_{ss}^{1/2})$ in the evaluation of $\langle t \rangle$. Similarly, we expand the exponentials of $V(\eta)/D(\eta)$ around ξ ,

$$\int_0^y d\xi \frac{V(\xi)}{D(\xi)} \int_0^\xi d\eta \frac{V(\eta)}{D(\eta)}$$

around y and

$$\int_0^x dy \frac{1}{V(y)} \int_0^y d\xi \frac{V(\xi)}{D(\xi)} \int_0^\xi d\eta \frac{V(\eta)}{D(\eta)}$$

around x for $x \in (5 \times 10^{-4}, I_{ss}^{1/2})$ in the evaluation of $\langle (\Delta t)^2 \rangle$.

For $5 \times 10^{-4} < x < I_{ss}^{1/2}$, the multiplicative noise term is dominant, and we may drop the additive noise. The cubic nonlinearity must now be included. Thus

$$F(x) \approx a_0 x - Ax^3 + \frac{1}{2} P' x \quad (5 \times 10^{-4} < x < I_{ss}^{1/2}) \quad (A24)$$

and

$$D(x) \approx \frac{1}{2} P' x^2 \quad (5 \times 10^{-4} < x < I_{ss}^{1/2}). \quad (A25)$$

From Eqs. (A13) and (A16) we get

$$\begin{aligned} & \int_{5 \times 10^{-4}}^{I_{ref}^{1/2}} dx \frac{1}{V(x)} \int_0^x dy \frac{V(y)}{D(y)} \\ & \approx \int_{5 \times 10^{-4}}^{I_{ref}^{1/2}} dx \frac{1 - \exp \left[-\frac{x}{D(x)} [F(x) - D'(x)] \right]}{[F(x) - D'(x)]}. \end{aligned} \quad (A26)$$

The exponential term in the above equation is very small compared to unity for the entire range of values of x and

$$\begin{aligned} & 4 \int_{5 \times 10^{-4}}^{I_{ref}^{1/2}} dx \frac{1}{V(x)} \int_0^x dy \frac{1}{V(y)} \int_0^y d\xi \frac{V(\xi)}{D(\xi)} \int_0^\xi d\eta \frac{V(\eta)}{D(\eta)} \\ & \approx \int_{5 \times 10^{-4}}^{I_{ref}^{1/2}} dx \frac{16P'}{x [16(a_0 - Ax^2)^3 - 60P'(a_0 - Ax^2)^2 + 8P'(a_0 - Ax^2)(5a_0 + 4P') - P'^2(24a_0 + P')]} \end{aligned} \quad (A31)$$

For typical values of the parameters we may neglect

$$[-60P'(a_0 - Ax^2)^2 + 8P'(a_0 - Ax^2)(5a_0 + 4P') - P'^2(24a_0 + P')]$$

in the denominator. Thus

$$\begin{aligned} & 4 \int_{5 \times 10^{-4}}^{I_{ref}^{1/2}} dx \frac{1}{V(x)} \int_0^x dy \frac{1}{V(y)} \int_0^y d\xi \frac{V(\xi)}{D(\xi)} \int_0^\xi d\eta \frac{V(\eta)}{D(\eta)} \approx \frac{P'}{2} \int_{2.5 \times 10^{-7}}^{I_{ref}} dz \frac{1}{z(a_0 - Az)^3} \\ & \approx \frac{P'}{2a_0^3} \left[\left(\frac{3}{2} - I_0 \right) / (1 - I_0)^2 + \ln \left[\frac{I_0}{1 - I_0} \right] - \frac{3}{2} \right. \\ & \quad \left. + \ln(4 \times 10^6) + \ln \left[\frac{a_0}{A} \right] \right]. \end{aligned} \quad (A32)$$

hence may be neglected without appreciable error. Thus

$$\begin{aligned} & \int_{5 \times 10^{-4}}^{I_{ref}^{1/2}} dx \frac{1}{V(x)} \int_0^x dy \frac{V(y)}{D(y)} \\ & \approx \frac{1}{2a_0} \left[-\ln(2.5 \times 10^{-7}) + \ln \left[\frac{a_0}{A} \right] + \ln \left[\frac{I_0}{1 - I_0} \right] \right]. \end{aligned} \quad (A27)$$

Combining Eqs. (A22) and (A27), we obtain

$$\langle t \rangle \approx \frac{1}{2a_0} \left[C + \ln \left[\frac{a_0^2}{PA} \right] + \ln \left[\frac{I_0}{1 - I_0} \right] \right], \quad (A28)$$

which is identical with Eq. (10). The presence of the multiplicative white noise has not appreciable effect on the mean first-passage time.

From Eqs. (A13), (A17), (A24), and (A25) we have

$$\begin{aligned} & \int_0^\xi d\eta \frac{V(\eta)}{D(\eta)} \\ & \approx e^{U(\xi) - \ln D(\xi)} \int_0^\xi d\eta \exp \left[(\eta - \xi) \left[U'(\xi) - \frac{D'(\xi)}{D(\xi)} \right] \right] \\ & \approx \frac{e^{U(\xi)}}{F(\xi) - D'(\xi)}, \end{aligned} \quad (A29)$$

where we drop the exponential term since $\exp\{-\xi[F(\xi) - D'(\xi)]/D(\xi)\} \ll 1$ for the entire range of ξ . Further, we obtain

$$\begin{aligned} & \int_0^y d\xi \frac{V(\xi)}{D(\xi)} \int_0^\xi d\eta \frac{V(\eta)}{D(\eta)} \\ & \approx \frac{4e^{2U(y)}}{y^2 [8(a_0 - Ay^2)^2 + 10AP'y^2 - P'(6a_0 - P')]} \end{aligned} \quad (A30)$$

and proceeding similarly

Combination of Eqs. (A23) and (A32) gives

$$\langle (\Delta t)^2 \rangle \simeq \frac{\pi^2}{24a_0^2} + \frac{P'}{2a_0^3} \left[\left(\frac{3}{2} - I_0 \right) \frac{1}{(1-I_0)^2} + \ln \left[\frac{I_0}{1-I_0} \right] - \frac{3}{2} + \ln(4 \times 10^6) + \ln \left[\frac{a_0}{A} \right] \right]. \quad (\text{A33})$$

Equations (A28) and (A33) give us the mean first-passage time and its variance for this model.

-
- ¹H. Haken, in *Encyclopedia of Physics*, edited by S. Flügge (Springer-Verlag, Berlin, 1970), Vol. XXV/2c.
- ²M. Sargent III, M. O. Scully, and W. E. Lamb, Jr., *Laser Physics* (Addison-Wesley, Reading, Mass., 1974).
- ³M. Lax, in *Brandeis Lectures*, edited by M. Chretien, E. P. Gross, and S. Deser (Gordon and Breach, New York, 1969), Vol. II.
- ⁴W. H. Louisell, *Quantum Statistical Properties of Radiation* (Wiley, New York, 1973).
- ⁵(a) F. T. Arecchi, V. Degiorgio, and B. Querzola, *Phys. Rev. Lett.* **19**, 1168 (1967); (b) F. T. Arecchi and V. Degiorgio, *Phys. Rev. A* **3**, 1108 (1971).
- ⁶(a) D. Meltzer and L. Mandel, *Phys. Rev. Lett.* **25**, 1151 (1970); (b) *Phys. Rev. A* **3**, 1763 (1971).
- ⁷K. Kaminishi, R. Roy, R. Short, and L. Mandel, *Phys. Rev. A* **24**, 370 (1981).
- ⁸R. Short, L. Mandel, and R. Roy, *Phys. Rev. Lett.* **49**, 647 (1982).
- ⁹R. Graham, M. Hohnerbach, and A. Schenzle, *Phys. Rev. Lett.* **48**, 1396 (1982).
- ¹⁰(a) A. Schenzle and R. Graham, *Phys. Lett.* **98A**, 319 (1983); (b) A. Schenzle, in *Optical Instabilities*, edited by R. W. Boyd, M. G. Raymer, and L. M. Narducci (Cambridge University Press, Cambridge, England, 1986).
- ¹¹(a) J. M. Sancho, M. San Miguel, S. Katz, and J. D. Gunton, *Phys. Rev. A* **26**, 1589 (1982); (b) A. Hernandez-Machado, M. San Miguel, and J. M. Sancho, *ibid.* **29**, 3388 (1984).
- ¹²A. Hernandez-Machado, M. San Miguel, and S. Katz, *Phys. Rev. A* **31**, 2362 (1985).
- ¹³S. N. Dixit and P. S. Sahni, *Phys. Rev. Lett.* **50**, 1273 (1983).
- ¹⁴R. F. Fox, G. E. James, and R. Roy, *Phys. Rev. Lett.* **52**, 1778 (1984).
- ¹⁵R. F. Fox, G. E. James, and R. Roy, *Phys. Rev. A* **30**, 2482 (1984).
- ¹⁶K. Lindenberg, B. J. West, and E. Cortes, *Appl. Phys. Lett.* **44**, 175 (1984).
- ¹⁷P. Jung and H. Risken, *Phys. Lett.* **103A**, 38 (1984).
- ¹⁸J. P. Gordon and E. W. Aslaksen, *IEEE J. Quantum Electron.* **QE-6**, 428 (1970).
- ¹⁹M. Suzuki, *J. Stat. Phys.* **16**, 477 (1977).
- ²⁰F. Haake, *Phys. Rev. Lett.* **41**, 1685 (1978).
- ²¹F. Haake, J. W. Haus, and R. J. Glauber, *Phys. Rev. A* **23**, 3255 (1981).
- ²²F. T. Arecchi and A. Politi, *Phys. Rev. Lett.* **45**, 1219 (1980).
- ²³F. T. Arecchi, A. Politi, and L. Ulivi, *Nuovo Cimento* **71**, 119 (1982).
- ²⁴M. R. Young and S. Singh, *Phys. Rev. A* **31**, 888 (1985).
- ²⁵F. de Pasquale, P. Tartaglia, and P. Tombesi, *Physica* **99A**, 581 (1979).
- ²⁶F. de Pasquale, P. Tartaglia, and P. Tombesi, *Z. Phys. B* **43**, 353 (1981).
- ²⁷D. Polder, M. Schuurmans, and Q. Vreken, *Phys. Rev. A* **19**, 1192 (1979).
- ²⁸P. Goy, L. Moi, M. Gross, J. M. Raimond, C. Fabre, and S. Haroche, *Phys. Rev. A* **27**, 2065 (1983).
- ²⁹E. Schrödinger, *Phys. Z.* **16**, 289 (1915).
- ³⁰H. A. Kramers, *Physica (Utrecht)* **7**, 284 (1940).
- ³¹D. A. Darling and A. J. F. Siegert, *Ann. Math. Stat.* **24**, 624 (1953).
- ³²E. W. Montroll and K. E. Shuler, *Adv. Chem. Phys.* **1**, 361 (1958).
- ³³R. Landauer and J. A. Swanson, *Phys. Rev.* **21**, 1668 (1961).
- ³⁴R. L. Stratonovich, *Topics in the Theory of Random Noise* (Gordon and Breach, New York, 1963).
- ³⁵G. H. Weiss, in *Stochastic Processes in Chemical Physics*, edited by I. Oppenheim, K. E. Shuler, and G. K. Weiss (MIT Press, Cambridge, Mass., 1977).
- ³⁶N. G. Van Kampen, *Stochastic Processes in Physics and Chemistry* (North-Holland, Amsterdam, 1982).
- ³⁷Z. Schuss, *Theory and Applications of Stochastic Differential Equations* (Wiley, New York, 1980).
- ³⁸C. W. Gardiner, *Handbook of Stochastic Methods* (Springer-Verlag, Berlin, 1983).
- ³⁹H. Risken, *The Fokker-Planck Equation* (Springer-Verlag, Berlin, 1984).
- ⁴⁰P. Hanggi, F. Marcheson, and P. Grigolini, *Z. Phys. B* **56**, 333 (1984).
- ⁴¹P. Hanggi, T. J. Mroczkowski, F. Moss, and P. V. E. McClintock, *Phys. Rev. A* **32**, 695 (1985).
- ⁴²R. F. Fox, *Phys. Rev. A* **33**, 467 (1986).
- ⁴³R. F. Fox, *Phys. Rev. A* (to be published).
- ⁴⁴J. Masoliver, K. Lindenberg, and B. J. West, *Phys. Rev. A* **33**, 2177 (1986).
- ⁴⁵(a) F. de Pasquale, J. M. Sancho, M. San Miguel, and P. Tartaglia, *Phys. Rev. A* **33**, 4360 (1986); (b) *Phys. Rev. Lett.* **56**, 2473 (1986).
- ⁴⁶R. Roy, A. W. Yu, and S. Zhu, *Phys. Rev. Lett.* **55**, 2794 (1985).
- ⁴⁷*Tables of Integrals, Series and Products*, edited by I. S. Gradshteyn and I. M. Ryzhik (Academic, New York, 1980).
- ⁴⁸A. J. F. Siegert, *Phys. Rev.* **81**, 617 (1951).
- ⁴⁹R. B. Schaefer and C. R. Willis, *Phys. Rev. A* **13**, 1874 (1976).
- ⁵⁰S. E. Miller, *IEEE J. Quantum Electron.* **QE-21**, 1644 (1985).
- ⁵¹S. E. Miller, *IEEE J. Quantum Electron.* **QE-22**, 16 (1986).
- ⁵²These multiple peaks in the FPT distributions have been observed in experiments in our laboratory.